Ammonia Gas Removal Using a Biotrickling Filter Coupled with an Anammox Bioreactor

by

Lauren Jean Frei

Department of Civil & Environmental Engineering
Duke University

Date:_____
Approved:

_____
Marc Deshusses, Supervisor

_____
Claudia Gunsch

_____
Lawrence David

Thesis submitted in partial fulfillment of
the requirements for the degree of Master of Science in the Department of
Civil & Environmental Engineering in the Graduate School
of Duke University

2018

ABSTRACT

Ammonia Gas Removal Using a Biotrickling Filter Coupled with an Anammox Bioreactor

by

Lauren Jean Frei

Department of Civil & Environmental Engineering
Duke University

Date:_____
Approved:

_____
Marc Deshusses, Supervisor

_____
Claudia Gunsch

_____
Lawrence David

An abstract of a thesis submitted in partial
fulfillment of the requirements for the degree
of Master of Science in the Department of
Civil & Environmental Engineering in the Graduate School of
Duke University

2018

Abstract

Ammonia is an odorous gaseous compound emitted by a variety of industrial facilities. This study aimed to address the feasibility of ammonia gas removal using a biotrickling filter (BTF) coupled with an anammox bioreactor. In the BTF, the influent ammonia gas partitioned into the trickling water and was converted to nitrite via partial nitrification. The effluent liquid from the BTF, containing nitrite and ammonium concentrations, was fed into the anammox reactor where autotrophic denitrifying bacteria converted the ammonium and nitrite to dinitrogen gas. For the anammox reactor to operate efficiently, the influent ammonium and nitrite concentrations must be in a 1 to 1 molar ratio. To evaluate the feasibility of this system, a lab scale BTF and anammox reactor were constructed and operated and a conceptual model for this system was developed. To obtain a nitrite to ammonium ratio close to 1, it was found that the effluent pH from the BTF must be maintained below 7, and the loading rate could not exceed 8.7 g N/m^3h. At this loading rate, complete ammonia gas removal occurred. A recycle rate of 1.4 times that of the influent was implemented in the BTF to increase performance and improve the nitrite to ammonium ratio. The addition of the recycle line achieved a nitrite of ammonium ratio of 0.97 at a pH value of 7.67. The anammox reactor achieved 88% removal of ammonium and nitrite at a loading rate of 10.5 g N /m^3h. The fact that the BTF was able to achieve a 1 to 1 nitrite to ammonium

ratio indicated that coupling of a BTF with the anammox reactor should be feasible. The mathematical model underpredicted effluent ammonium and nitrite concentrations in the BTF and greatly overpredicted the effluent concentrations from the anammox reactor. To improve the BTF model inhibition factors and oxygen supply need to be accounted for. Further development of the growth kinetics in the annamox model are necessary as well.

Contents

List of Tables

List of Figures

1. Introduction

Ammonia is an odorous gas produced by composting facilities (Melse, R.W; Ogink, 2005), fertilizer manufacturing, swine and poultry production (Sakuma, Jinsiriwanit, Hattori, & Deshusses, 2008), wastewater treatment facilities and chemical manufacturing facilities (Moussavi, Khavanin, & Sharifi, 2011). Ammonia gas emissions can cause odor nuisance, and well as many environmental issues, especially in aquatic ecosystems since it is toxic to vertebrates (Randall & Tsui, 2002). Various treatment processes exist for removing ammonia gas. Chemical scrubbers, a common physical/chemical treatment process for ammonia gas removal can remove over 90 % of ammonia gas (Melse, R.W; Ogink, 2005). However, chemical scrubbers do not remove ammonia gas odor as well as biological filters (Xue, Wang, Wu, Sun, & Xie, 2010). Additionally, chemical scrubbers produce large amounts of acidic ammonium solution that requires proper disposal (Sakuma et al., 2008).

Biological treatment is another treatment alternative for ammonia gas removal. Biological treatment uses ammonium oxidizing bacteria (AOB) to convert ammonium to nitrite and nitrite oxidizing bacteria (NOB) to convert nitrite to nitrate. Biofilters and biotrickling filters (BTFs) are two common biotechnologies for the treatment of odorous air. Traditional biofilters use compost and woodchips, peat or soil as packed solids for bacterial attachment, nutrients supply and to provide pH buffer. In biofilters, ammonia is absorbed into the damp surface, transferred to the bacterial cells and then converted

to nitrite and nitrate by nitrifying bacteria. However, biofilters can accumulate ammonium, nitrite or nitrate which can lead to inhibition of the nitrifying communities present in the bioreactor (Moussavi et al., 2011). Unlike a biofilter, a BTF has liquid running through the reactor, thus providing a means to eliminate this problem. The inert packing materials (e.g., polyurethane foam, plastic support, or porous ceramics) in BTFs are only supporting carriers for bacterial growth. Nutrient supply and pH buffering are achieved through the liquid or mineral medium trickling and recirculation. Ammonia dissolved in the liquid phase is oxidized to nitrite and nitrate in BTFs, which facilitates further dissolution of ammonia and thus reduces fresh water replacement in comparison with chemical scrubbers. However, the resulting effluent water from BTFs has a high nitrogen concentration which can be problematic for discharge as nitrite and nitrate are still important culprits for aquatic eutrophication. To address this problem a denitrification system is often added after the nitrification process in the BTF.

A study was conducted on removing ammonia from a gas stream using a simultaneous nitrification/denitrification (SND) BTF system. In a SND system, nitrification and denitrification occur in a single biofilm reactor. The nitrification process occurs in the outer aerobic layers of the biofilm while the denitrification process occurs in the inner anaerobic layers. Maintaining a constant empty bed residence time (EBRT) of 60 seconds, this study tested various influent ammonia concentrations. The tested ammonia concentrations of 100 ppm, 200 ppm, 300 ppm, 400 ppm and 600 ppm

achieved removal rates of 100%, 97.8%, 96.7%, 91.7% and 73.6%, respectively. The study found that a 91% removal rate occurred when the loading of the reactor was 14 g N/m^3h. However loading rates higher than this resulted in a decrease in removal rate due to limitation in the biofilm (Moussavi et al., 2011).

Another study conducted by Sakuma et al. focused on the use of a BTF and a post denitrification system to remove ammonia from an air stream. In this study ammonia concentrations in the influent gas stream ranged from 270 to 700 ppm at an EBRT of 13.5 seconds. Complete removal was achieved at loadings of 56 g/m^3h and the critical load – load at which 95% of removal occurred- was found to be 66 g/m^3h. This critical load was higher than those found by other biofiltration studies. Most studies have found the critical load to range between 5 and 40 g NH_3/m^3h (Sakuma et al., 2008).

Both the studies conducted by Moussavi et al. and Sakuma et al. demonstrated that nitrification in a BTF coupled with a denitrification process can successfully treat an air stream containing ammonia. However, while nitrification coupled with denitrification can successfully remove ammonia from a gas stream, it typically requires an external electron donor source (Moussavi et al., 2011). The anaerobic ammonium oxidation (anammox) process is a relatively recent discovered biological process that can convert ammonia and nitrite to dinitrogen gas and water. The use of an anammox system rather than a denitrification can result in a 90% operating cost reduction as no external electron donor source is needed and less biomass is produced(Sri Shalini S &

Joseph, 2014). In the anammox reaction, ammonium is oxidized with nitrite as the electron acceptor in a one to one molar ratio to anaerobically produce dinitrogen gas and water (Niftrik, Fuerst, & Damst, 2004). The reaction is provided in Equation 1 below:

$$NH_4^+ + NO_2^- \rightarrow N_2 + 2H_2O \quad (1).$$

Unlike heterotrophic denitrification, the anammox process does not require an additional carbon source as electron donor, and produces less biomass (Chen et al., 2017). The anammox process has been coupled with the Single Reactor High Activity Ammonia Removal Over Nitrite (SHARON) process to remove ammonia from water. The SHARON process reduces ammonia to nitrite via ammonia oxidizing bacteria (AOB). Ideally the SHARON process creates a 1:1 ammonium to nitrite ratio to be fed into the anammox reactor. Once in the anammox reactor, the anammox bacteria convert the ammonium and nitrite to dinitrogen gas and water (Chen et al., 2017).

In this study, BTF was coupled with an anammox reactor to remove ammonia from an airstream by completely converting it to dinitrogen gas. This system was studied using a lab scale BTF and anammox reactor. The BTF served to absorb the influent ammonia and partially nitrify it to nitrite so that the trickling liquid can then be fed to the anammox reactor for autotrophic denitrification, thereby regenerating the trickling liquid. This research aimed to demonstrate the feasibility of this concept for the treatment of ammonia contaminated air streams.

Additionally, a conceptual model of the process was developed and solved numerically. The model aimed to accurately represent the different treatment steps through the development of appropriate mass balances for ammonia and nitrite in the BTF and in the anammox bioreactors.

2. Laboratory Study of the Coupling of a Biotrickling Filter and an Anammox Reactor

2.1 Introduction

To experimentally determine the feasibility of the coupling of a BTF and anammox reactor for the complete treatment of low concentrations of ammonia air streams, a lab scale BTF and anammox reactor were constructed and operated. In the lab scale reactor system, ammonia was removed from a synthetic waste air stream through the sequence of absorption and partial nitrification in a BTF followed by autotrophic denitrification in an anammox bioreactor configured as an up flow anaerobic sludge blanket (UASB) reactor. For the BTF-anammox coupled system to operate efficiently, the nitrite to ammonium ratio must be equal to 1. Thus, experiments were conducted to determine the optimum operational parameters (pH, ammonia loading, liquid recycle rate). Additionally, the overall performance of the BTF and anammox bioreactors was evaluated.

2.2 Materials and Methods

2.2.1 Biotrickling Filter Nitration Setup and Operation

The BTF consisted of a 0.1 m. diameter 1.5 m. tall clear PVC column packed with 4 cm polyurethane foam cubes (interfacial area of 600 m^2 m^{-3}) to a height of 1.2 m to serve as support for the nitrifying biofilm growth. Biofilm cultivation was conducted in batch mode for 11 days prior to the experiment. 3.5 L of pig farm wastewater was added to the BTF and continuously recirculated at a rate of 5 L/h until more than 90% ammonium in the wastewater was reduced. After a first batch of 7 days, air was introduced to the BTF during the second and third batches to supply sufficient oxygen for ammonium oxidation and biofilm growth.

After the startup phase, synthetic waste air was prepared by mixing humidified compressed air and pure ammonia gas to reach the desired concentrations (50-450 ppm_v). The ammonia gas flow was controlled by an Alicat Scientific mass flow controller (located on the upper shelf of the reactor system) while the air stream flowrate was set using a simple flow meter (Dwyer, attached to the support frame of the reactor system). The synthetic contaminated air stream flowed co-currently with the trickling liquid from the top of the BTF. The trickling liquid contained 0.3 g/L of $NaHCO_3$, 0.3 g/L of KH_2PO_4, 0.025 g/L of $CaCl_2$, and 0.05 g/L of $MgSO_4$ $7H_2O$. The influent pH was adjusted using a 2.5 M NaOH solution so that it ranged between 6.45 and 6.55. The influent and effluent liquid flow rates (10 to 20 L/d depending on the experiment) were

controlled by a peristaltic pump. The BTF was originally operated as a one pass for the liquid. After 231 days of operation, a liquid recycle line was added to the BTF in an attempt to improve nitrification. The trickling recycle was achieved by a peristaltic pump diverting a portion of the effluent flow back to the top of the BTF. The recycle flowrate ranged from 3 L/d to approximately 42 L/d to determine the impact of the recycle rate.

2.2.2 Anammox Reactor Setup and Operation

The anammox reactor consisted of two clear PVC pipes connected with a connector. The upper section had an inner diameter of 0.2 m. and was 0.5 m. tall. The lower section had an inner diameter of 0.1 m. and was 0.6 meters tall. Due to the slow growth rate of anammox bacteria, the anammox reactor was filled with anammox bacteria grown on circular packing (2.5 cm diameter) from the South Durham Wastewater Treatment Facility (Durham, NC). This eliminated a lengthy startup phase.

Although the intent is to couple the BTF and anammox bioreactors and operate them as one system, the two bioreactors where started and operated separately for most of this study. The anammox bioreactor was fed liquid containing mineral medium similar to the BTF trickling liquid spiked with ammonium and nitrite. Feeding was from the bottom of the reactor at flow rates ranging from 7 L/d to 16 L/d using a peristaltic pump. The mineral medium consisted of 0.01 g/L of KH_2PO_4, 0.005 g/L of $CaCl_2$, 0.3 g/L

of $MgSO_4$ $7H_2O$ and 1.25 g/L of $NaHCO_3$. The influent pH was adjusted using 1 M H_2SO_4 solution to range between 6.9 and 7.0.

2.2.3 Analytical Methods

To determine the performance of the BTF and anammox reactor, gas and water samples were routinely collected and analyzed. Water samples were collected from the bottom of the BTF and influent and effluent of the anammox reactor. The aqueous samples were diluted with deionized (DI) water and analyzed for ammonium, nitrate and $nitrite^-$ using Hach kits (AmVer High Range Ammonia Reagent Set for ammonia/ammonium, Nitraver X reagent for nitrate and Spectroquant Nitrite Kit for nitrite). The BTF influent trickling was not tested as it did not contain any nitrogen species. The influent and effluent pH was measured by collecting influent and effluent water samples and using a bench top pH probe (Oakton). The influent and effluent ammonia gas concentrations for the BTF were determined using a photoionization detector (PID) (RAE). The influent ammonia concentration in the air stream was measured by connecting a small knock out jar to the influent air line and inserting the PID into the effluent air line from this knock out jar. The effluent ammonia concentration in the air stream was measured by inserting the PID into the effluent gas line from the BTF. A knock out jar was not necessary as a knock jar was already present in the reactor configuration. A calibration curve was developed using known

concentrations. Using the gas and liquid data the ammonia and nitrite loading, removal and elimination capacity, were determined for the BTF and anammox reactor.

2.3 Results and Discussion

2.3.1 Biotrickling Filter Reactor Performance

To evaluate the performance of the BTF, effluent water samples were collected and analyzed for ammonium/ammonia, nitrite and nitrate using Hach kits. Ammonium and nitrite were the primary constituents in the effluent water indicating high activity of AOB and low activity of NOB. Concentrations of nitrate were detected but these concentrations were relatively low compared to that of nitrite and ammonium. Effluent nitrite, ammonium and nitrate concentrations are provided in Figure 1 below with the reactor loading.

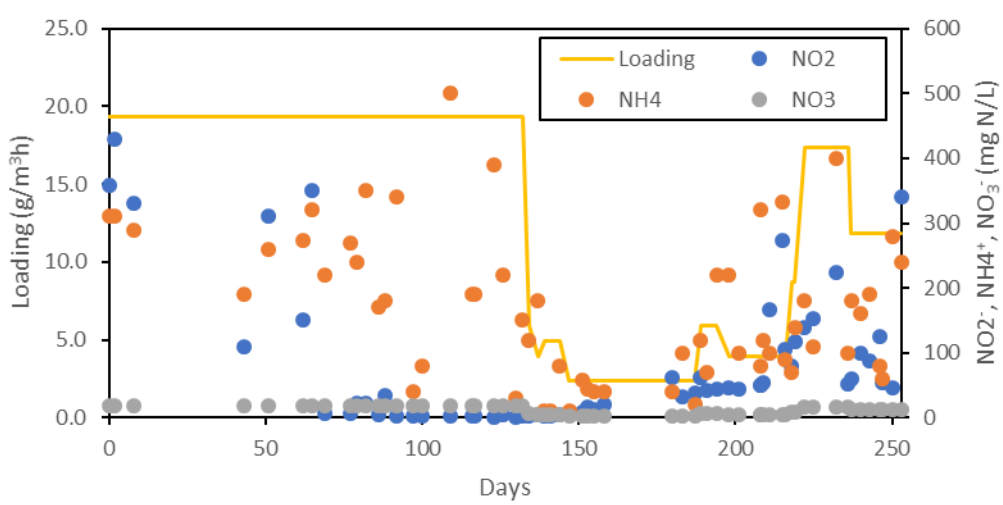

Figure 1: Effluent nitrite, ammonium and nitrate concentrations and reactor loading

The effluent ammonium, nitrite and nitrate concentrations ranged from 10 to 390 mg N/L, 2 to 430 mg N/L, and 1 to 42 mg/L, respectively. The wide variation in the concentrations was a result from reactor loading and reactor sensitivity to the resulting loading. The loading ranged from 2.4 to 19.3 g/m^{3}h. A similar study conducted by Sakuma et al. found the effluent nitrite and nitrate concentrations to range from 25 to 100 g N/m^3 and low ammonium concentrations. In this study, the objective was to achieve complete nitrification in the BTF, therefore the low ammonium concentrations were desired. Additionally, the effluent nitrite and nitrate concentrations were higher as the loading rate to the BTF was higher in their study. The loading rate ranged from 56 g/m^{3}h to 120 g/m^{3}h (Sakuma et al., 2008).

To evaluate reactor performance of the BTF, the removal percentage of nitrogen and the elimination capacity (EC) were calculated and compared to the loading (Figure 2).

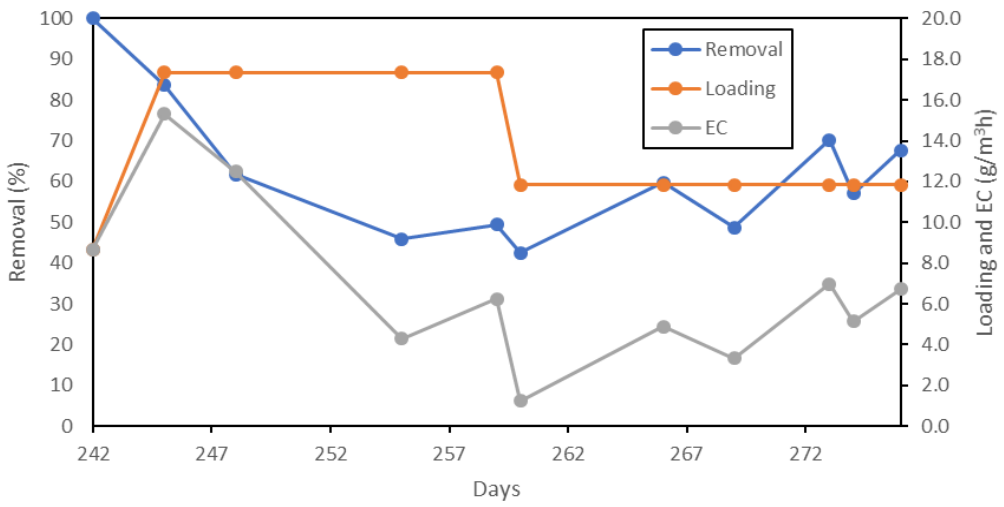

Figure 2: Biotrickling filter loading and its impact on ammonia gas removal and elimination capacity (EC).

At loadings below 8.7 g/m^{3}h, complete ammonia gas removal was achieved. It should also be noted that this loading rate resulted in a nitrite to ammonia ratio close to 1. At removal rates greater than 8.7 g/m^{3}h, the removal and EC decreased. At higher tested loadings of 17.4 g/m^{3}h and 11.8 g/m^{3}h the resulting removal rates were 60.15% ± 7% and 50.3% ± 8.7%. Compared to a study conducted by Sakuma et al. (Sakuma et al., 2008), these removal rates are low. Sakuma et al. achieved complete ammonia gas removal in their porous ceramic bead packed BTF for loading rates below 56 g/m^{3}h (Sakuma et al., 2008). However, Sakuma et al. were able to achieve significantly higher removal rates than most studies. For most studies, the critical loading rate ranged from 5 to 40 g/m^{3}h of ammonia gas (Sakuma et al., 2008). In the present study, the ammonia elimination capacity may have been low due to the pH issues observed when operating

at higher loading rates. Typically, nitrification reduces pH allowing it to counter the pH increase caused by ammonia absorption. However, this was not fully achieved in this study as increases in loading resulted in pH increases which negatively impacted nitrification.

2.3.2 Nitrite to ammonium ratio in the biotrickling filter

After initial startup, the influence operating parameters (pH and recycle rate) on the nitrite to ammonium ratio in the BTF were investigated. The nitrite to ammonium ratio was of key interest as ideally it must be as close to 1 for optimal efficiency of the anammox reactor. If ammonium or nitrite are in excess complete removal of nitrogen species in the liquid phase will not be possible. Additionally, if nitrite is in excess, the risk of nitrite inhibition becomes problematic. The influent pH was maintained at approximately 6.5. The resulting effluent pH from the BTF increased. The amount of increase depended on the mineral medium composition and the loading of the reactor. This increase in pH was surprising. Typically, nitrification reduces pH as bicarbonate is converted to carbonic acid. A pH increase resulted in less of the ammonia being converted to ammonium given the pKa value of ammonium, 9.25 (Benjamin, Mark, 2010). From days 74 to 102 of the experiment, the pH in the BTF exceeded the pKa value, indicating that ammonia was more prevalent than ammonium. The relationship between the effluent pH and the nitrite to ammonium ratio is shown in Figure 3. When pH values exceeded 9, the nitrite to ammonium ratio decreased dramatically as this pH

was too high for the AOB to function and less of the influent ammonia was converted to ammonium for nitrification.

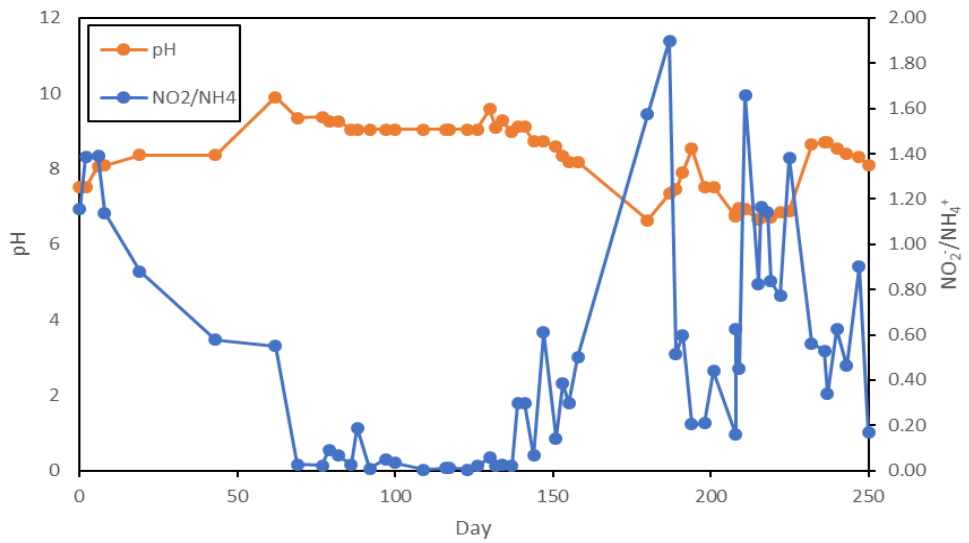

Figure 3: The influence of effluent pH on the nitrite to ammonium ratio.

To better identify the trend between pH and the nitrite to ammonium ratio, pH values above 9, between 8 and 9, between 7 and 8, and below 7 were averaged. Their respective nitrite to ammonium ratios were averaged as well and plotted against the average pH values (Figure 4).

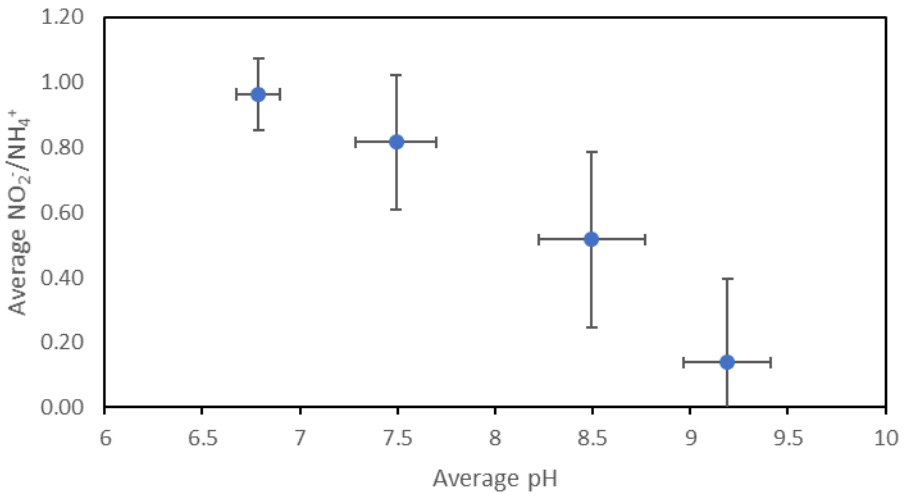

Figure 4: Average nitrite to ammonium ratio versus average pH

They reveal that the optimum effluent pH is below 7. pH values above 7 resulted in greatly decreased nitrification. A study conducted by Groeneweg et al. (Groeneweg, Sellner, & Tappe, 1994) in a batch bioreactor specifically looked at the influence of pH on the rate of ammonia oxidation and found that the maximum rate of ammonia oxidation occurred at pH values between 6.7 and 7. pH values outside this range resulted in a lower rate of ammonia oxidation (Groeneweg et al., 1994). These results were surprising as most other studies found the optimum pH to be 7.5 (Ramírez, Gómez, Aroca, & Cantero, 2009).

Maintaining the effluent pH below 7 depended on the ammonia loading and mineral medium in the influent liquid. The change in loading and corresponding change in pH are shown in Figure 5. The original mineral medium contained high salt concentrations (to serve as pH buffer) but this resulted in significant salt precipitation

inside the bed and clogging in the BTF which negatively impacted performance. On day 69 the mineral medium was significantly altered by decreasing the amount of sodium bicarbonate and potassium phosphate to address the salt formation and resulting clogging issues in the BTF. This change is indicated on Figure 5 by the red line. However, this change resulted in an increase in pH which negatively impacted the nitrite to ammonium ratio. On day 153 the amount of sodium bicarbonate and potassium phosphate in the mineral medium was increased and the loading to the BTF was decreased in an attempt to address the high pH issue. This change is indicated on Figure 5 by the yellow line after which a lower pH and improved nitrite to ammonium ratio were observed.

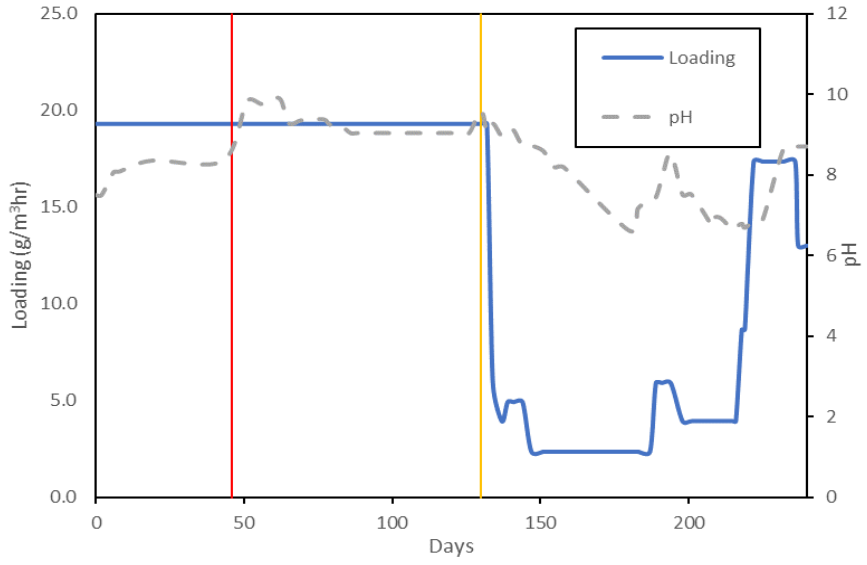

Figure 5: The impact of loading and mineral medium on the effluent pH in the BTF. See text for details of the changes with time.

The influence of reactor loading on the nitrite to ammonium ratio was also investigated. Loading ranged from 2.4 g/m^{3}h to 19.3 g/m^{3}h (Figure 6). Higher ammonia loading resulted in a reduced nitrite to ammonium ratio as high loading rates correlated with high pH values, increased absorption of ammonia and reduced nitrification. The optimal loading to achieve a nitrite to ammonium ratio close to 1 was 8.7 g/m^{3}h. Loadings rates below 8.7 g/m^{3}h resulted in a nitrite to ammonium ratio well below 1. This occurred as the low loading rates followed the high loading rates in which the BTF was not very active.

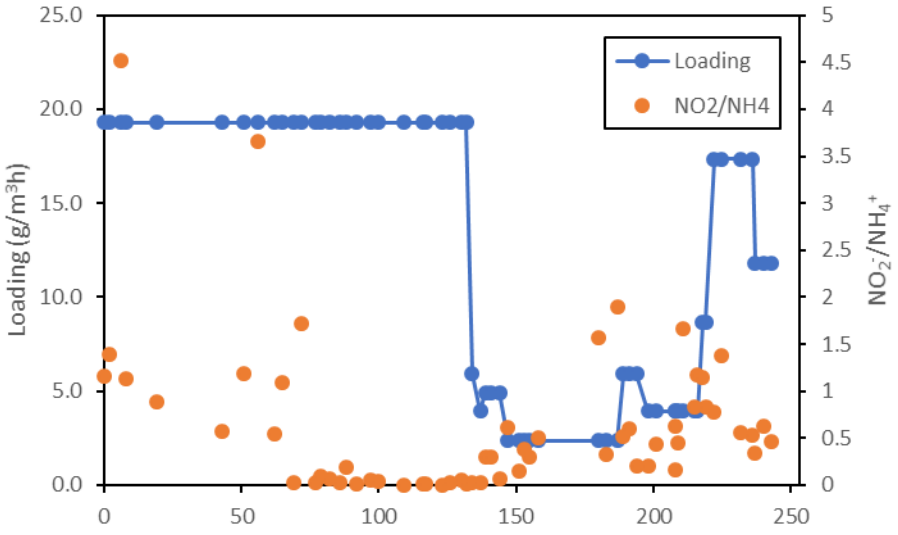

Figure 6: The influence of loading on the nitrite to ammonium ratio.

To better evaluate the impact of the loading rate on the nitrite to ammonium ratio, the loading rate was compared to the nitrification rate (i.e the amount of nitrite produced) as shown in Figure 7.

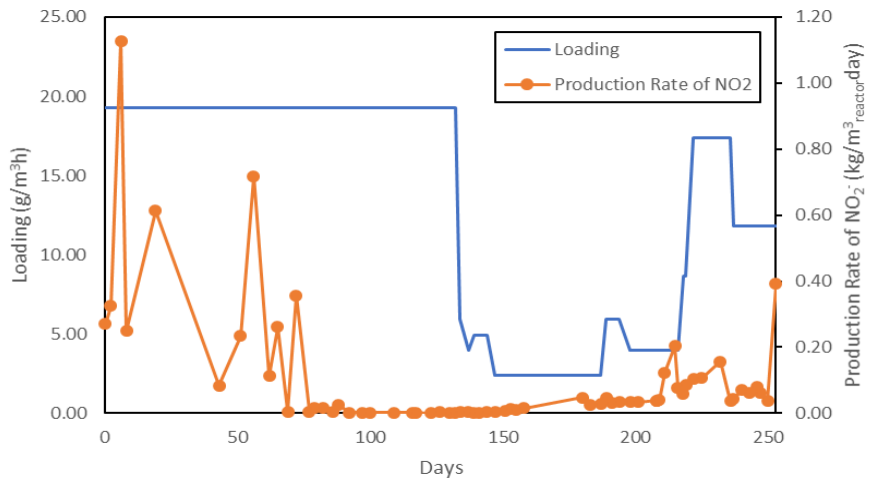

Figure 7: The influence of loading rate on the nitrite production rate

As shown in Figure 7, the nitrite production rate decreased at the high loading rate of 19.3 g/m^{3}h. To improve the nitrite production rate (and thus improve the nitrite to ammonium ratio), the reactor loading was significantly decreased to 5.9 g/m^{3}h on day 134 and further decreased to 2.4 g/m^{3}h on day 147. After the AOB had time to respond to the reduced loading rate, the nitrification rate increased.

To better control the effluent pH and to try improving the performance of the BTF, a recycle line was added on day 208. The trickling liquid recycle increased packing wetting and modified the axial distribution of ammonium in the liquid.

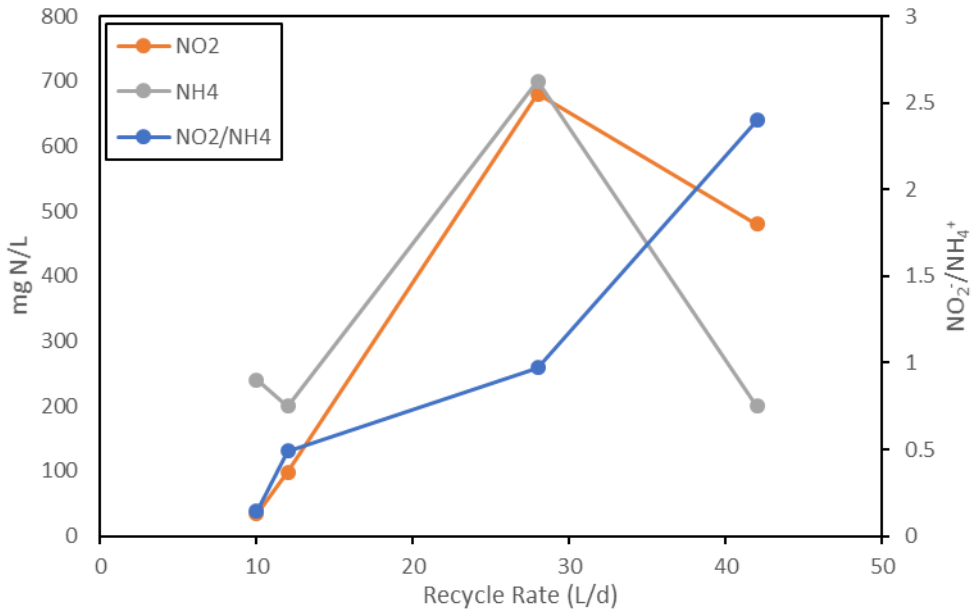

Figure 8: Ammonium and nitrite concentrations and the resulting nitrite to ammonium ratio at different recycle flow rates.

The results (Figure 8) show that a recycle rate of 28 L/d (approximately 1.4 times that of influent liquid mineral medium rate) corresponding to a trickling velocity of 0.16 m/h was necessary to achieve a nitrite to ammonium ratio close to 1. At lower recycle rates, the nitrite to ammonium ratio was below 1, indicating lower nitrification rates. However, at the highest recycle rates, the nitrite to ammonium ratio exceeded 1 indicating that more of the ammonium was oxidized to nitrite. As expected, this increased nitrification resulted in a lower pH as the recycle rate increased (Figure 9.). The increased recycle also appeared to enable greater nitrification at pH around 7.5, which was not the case when liquid was in a one pass mode.

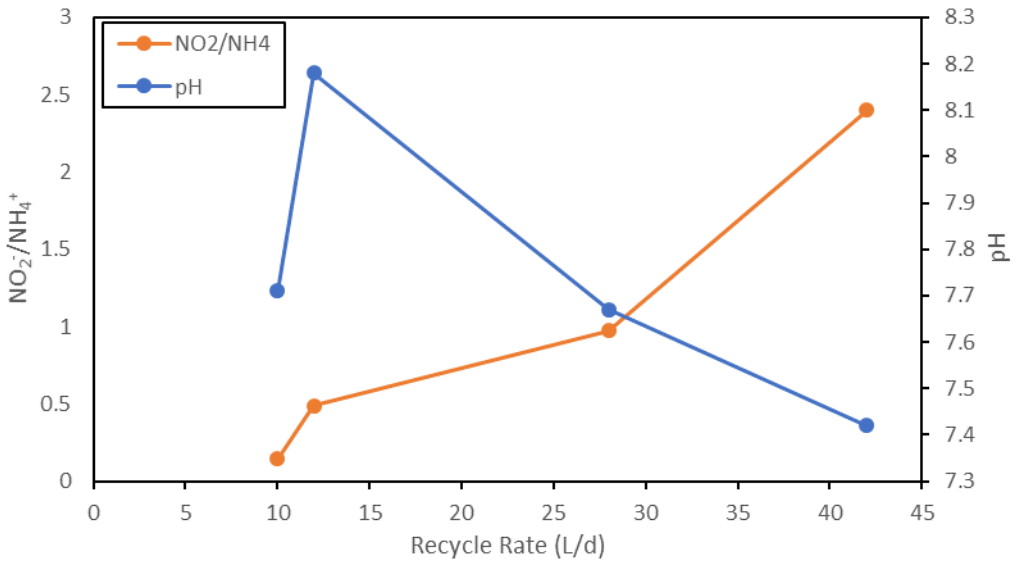

Figure 9: The influence of recycle rate on effluent pH and nitrite to ammonium ratio.

2.3.3 Anammox Reactor Performance

The anammox reactor was fed a liquid containing mineral medium, ammonium and nitrite since it was not connected to the BTF. The influent and effluent ammonium and nitrite concentrations are provided in Figure 10.

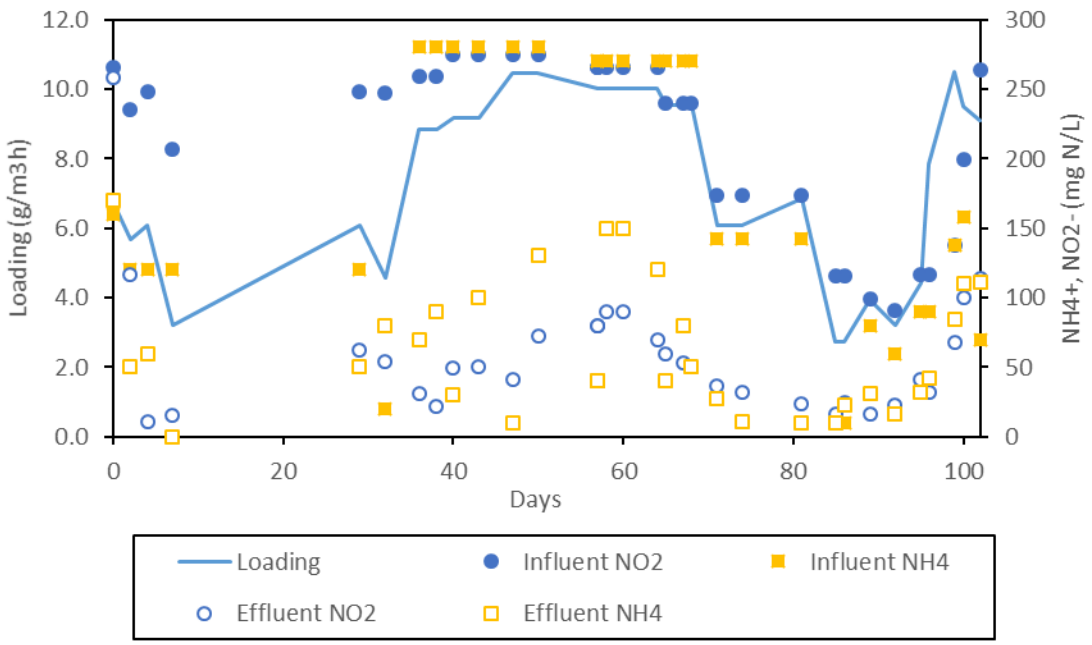

Figure 10: Anammox reactor loading and influent and effluent nitrite and ammonium concentrations

As shown in Figure 10, the anammox reactor was able to reduce the concentration of ammonium and nitrite. The largest reduction occurred on day 47 where ammonium and nitrite concentrations were reduced by 270 mg/L and 234 mg/L, respectively. The loading was 10.5 g/m^{3}h.

The performance of the anammox bioreactor is reported in Figure 11. Nitrogen removal efficiency was calculated using the influent and effluent ammonium, nitrite and nitrate concentrations.

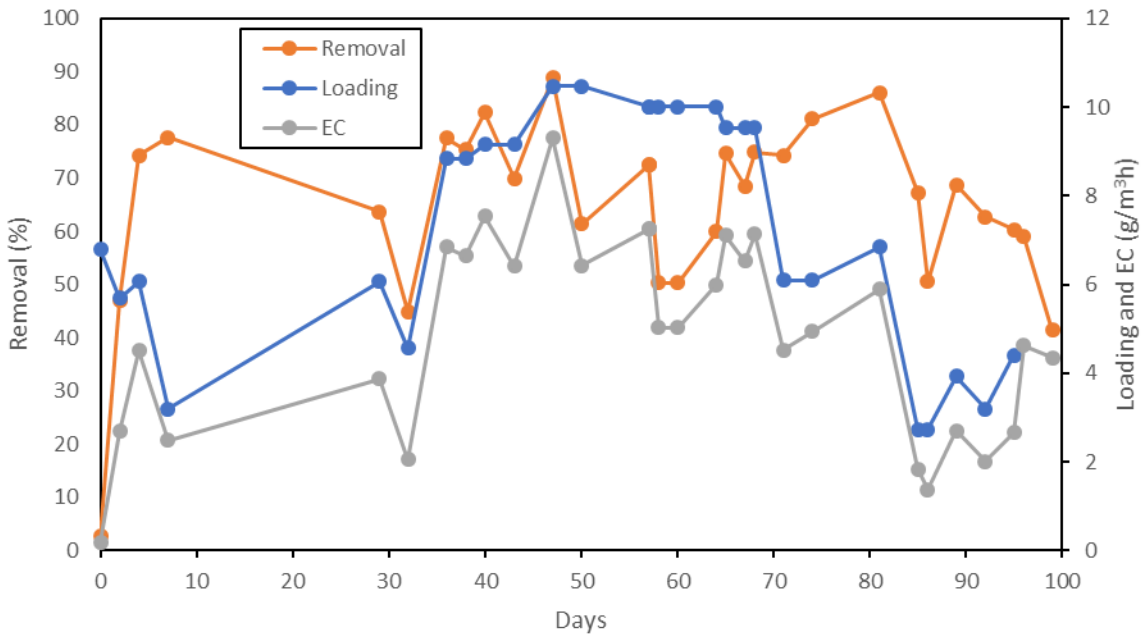

Figure 11: Anammox reactor loading influence on removal and elimination capacity (EC).

The corresponding denitrification rate (0.19 kg N/$m^3_{reactor}$day) is lower than reported in studies which have achieved combined ammonium and nitrite removal rates of 1.8 kg N/$m^3_{reactor}$ day (Marc Strous, Van Gerven, Zheng, Kuenen, & Jetten, 1997). Lower denitrification rates may have resulted for a variety of reasons. In the study conducted by Strous et al. the reactor included a recycle line to prevent high influent nitrite concentrations at the bottom of the reactor. For anammox bacteria high nitrite concentrations can be inhibitory. Additionally, Strous et al. took great measures to prevent any oxygen diffusion into the system. All tubing and connectors were made

from butyl rubber, norprene or polyvinylchloride. The influence of loading on the nitrification rate calculated for this study can be found in Figure 12.

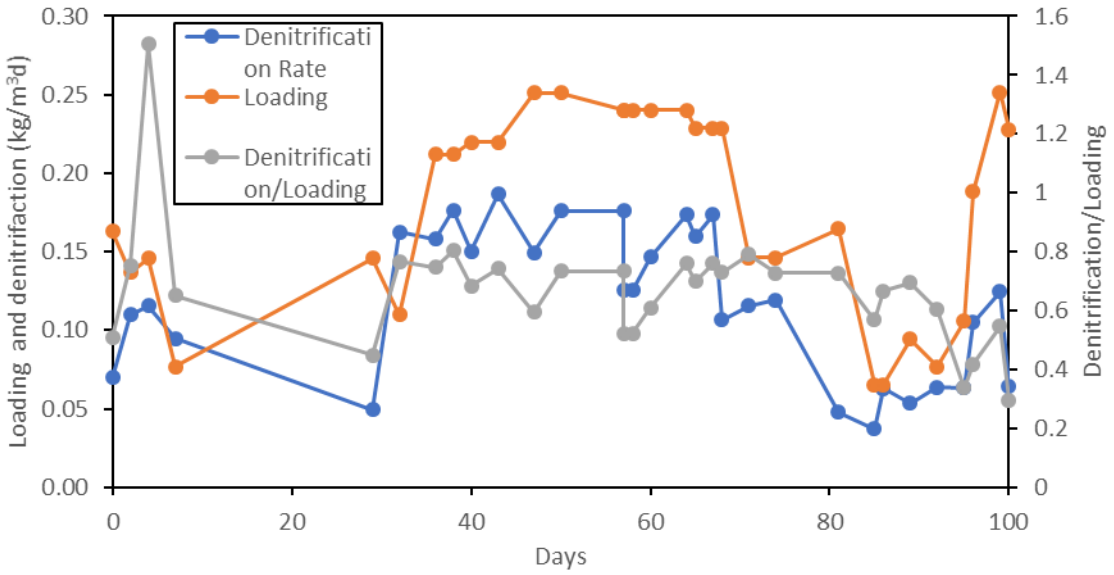

Figure 12: The influence of anammox reactor loading on the denitrification rate

As shown in both Figure 11 and Figure 12, the removal rate and nitrification rate were higher at higher loading rates. The highest denitrification rate (0.19 kg N/$m^3_{reactor}$day), removal rate (88%) and EC (9.3 gN/m^3hr) were achieved on day 47 when loading was 10.5 g/m^3h. Initially it was hypothesized that the removal efficiency, EC and denitrification rate would be highest at lower loading rates and decrease as the loading rate increased as other studies have found (Ramírez et al., 2009). The first increase in removal efficiency, EC and denitrification as the loading increase may have resulted from an increase in anammox bacteria. The anammox reactor was started on day 0. The initial denitrification rate, removal efficiency and EC were all very low, which was

expected. On day 4, the denitrification rate, removal efficiency and EC all increased as the anammox bacteria adjusted to the reactor. Anammox bacteria have a very slow growth rate, the doubling time is approximately 14 days. Therefore, an increase in denitrification, removal efficiency and EC after 14 days of operation may be due to an increase in anammox bacteria.

3. Model Development of the Coupling of a Biotrickling Filter and Anammox Bioreactor

3.1 Introduction

To better understand the coupling of a BTF with an anammox bioreactor and to maximize the efficiency of experimental testing, a conceptual model of the two bioreactors was developed in Berkeley Madonna, a modeling software. The objective of the model development was to determine operating parameters so that the BTF effluent contained equal amounts of ammonium and nitrite, and to determine the optimum design and operating criteria to achieve maximum ammonia gas removal from the overall system. The results from the model were compared to those collected from a lab scale BTF and anammox reactor system.

3.2 Model Development

3.2.1 Overview

The model consisted of two separate components, the BTF and the anammox reactor. Ammonia gas in air and liquid containing a mineral medium served as the inputs to the BTF and each stream (flowrate and concentrations) could be adjusted. When the models of the two bioreactors were joined, the outputs from the BTF, ammonium and nitrite, serve as input to the anammox reactor. The amount of ammonium and nitrite entering the anammox reactor could be adjusted through the liquid feed rate. Once in the anammox reactor, anaerobic microbes converted the ammonium, and nitrite to dinitrogen gas. The purpose of the model was to better understand the coupling of the BTF and the anammox reactor – specifically looking at the ammonium and nitrite concentrations in the liquid and biofilm throughout the process and support the optimization of the system.

3.2.2 Biotrickling Filter Model Development

To develop a model representing the BTF the following assumptions were made:

1. There are no nitrite oxidizers, therefore no nitrate is produced. This assumption is supported by our experiments which showed that only negligible concentrations of nitrate.
2. There is an unlimited supply of oxygen, therefore oxygen is not a limiting factor

3. The gas and liquid phases can be discretized in space and each of the differential gaseous or liquid element is considered as being ideally mixed
4. Bacterial growth is neglected resulting in the ammonium oxidation kinetics to be simplified to Michaelis-Menten type reaction kinetic. This is warranted as ammonia oxidizing bacteria are very slow growing organisms.
5. An interface layer exists between the liquid and biofilm layer
6. Mass transfer in gas, liquid and interface segments are governed by mass transfer coefficients
7. There is no inhibition associated with the development of free nitrous acid (FNA)

Mass balances were developed for the gas, liquid, interface and biofilm phase in the BTF and for the liquid, interface and biofilm phase for the anammox reactor. Figure 13 below depicts a mass balance schematic for both reactors.

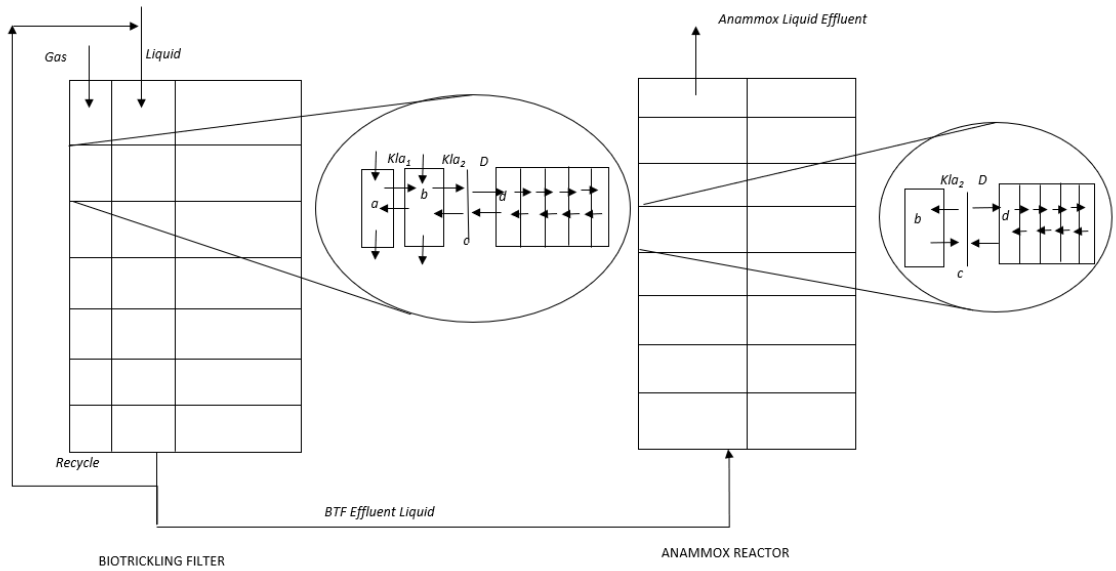

Reference Variable	Value
a	Gas
b	Liquid
c	Interface
d	Biofilm
Kla_1	Gas Mass Transfer Coefficient
Kla_2	Liquid Mass Transfer Coefficient
D	Diffusion

Figure 13: Mass balance schematic for the BTF and the anammox reactor.

As seen in Figure 13, air contaminated with traces of ammonia entered at the top of the BTF. In the BTF, as the air passed through the reactor, some of the ammonia partitioned into the trickling liquid layer as determined by Henry's Law and a gas mass transfer coefficient, Kla_1. Once in the liquid layer, the dissolved ammonia was converted

to aqueous ammonium. The aqueous ammonium either trickled down the liquid column or it transferred into the biofilm via diffusion described by Fick's law and a diffusivity coefficient D. Once in the biofilm, the ammonium was converted to nitrite through AOB. Using the schematic depicted in Figure 13 and the listed assumptions, dynamic mass balances for the gas phase, liquid phase, interface and biofilm were developed as shown in Equations 2 through 15 below. Note that in the developed equations, i refers to the vertical segment along the height of the BTF and j refers to the segment along the depth of the biofilm (depicted horizontally in Figure 13). The model equations use the array notations, i.e., [2..w] indicates that the equation is for i being equal to 2 all the way to w. All parameters referenced in the following equations can be found in Table 1 below.

Gas Mass Balance Equations:

$$\frac{d}{dt}(C[1]) = \frac{G}{E \cdot Vw} \cdot (C_{inlet} - C[1]) - \frac{Kla_1}{E} \cdot (\frac{C[i]}{kH} - Cl_{NH4}[i]) \quad (2)$$

$$\frac{d}{dt}(C[2..w]) = \frac{G}{E \cdot Vw} \cdot (C[i-1] - C[1]) - \frac{Kla_1}{E} \cdot (\frac{C[i]}{kH} - Cl_{NH4}[i]) \quad (3)$$

Liquid Mass Balance Equations:

$$\frac{d}{dt}(Cl_{NH4}[1]) = \left(\frac{L_{BTF}}{Vlw} \cdot (Influent_{NH4} - Cl_{NH4}[i]) + Kla_1 \cdot \left(\frac{C[i]}{kH} - Cl_{NH4}[i]\right) \cdot Vw - Kla_2 \cdot Vw \cdot (Cl_{NH4}[i] - Cl_{NH4-int}[i])\right) \quad (4)$$

$$\frac{d}{dt}(Cl_{NH4}[2..w]) = \left(\frac{L_{BTF}}{Vlw} \cdot (Cl_{NH4}[i-1] - Cl_{NH4}[i]) + Kla_1 \cdot \left(\frac{C[i]}{kH} - Cl_{NH4}[i]\right) \cdot Vw - Kla_2 \cdot Vw \cdot (Cl_{NH4}[i] - Cl_{NH4-int}[i])\right) \quad (5)$$

$$\frac{d}{dt}(Cl_{NO2}[1]) = \left(\frac{L_{BTF}}{Vlw} \cdot (Influent_{NO2} - Cl_{NO2}[i]) - Kla_2 \cdot Vw \cdot (Cl_{NO2}[i] - Cl_{NO2-int}[i])\right) \quad (6)$$

$$\frac{d}{dt}(Cl_{NO2}[2..w]) = \left(\frac{L_{BTF}}{Vlw} \cdot (Cl_{NO2}[i-1] - Cl_{NO2}[i]) - Kla_2 \cdot Vw \cdot (Cl_{NO2}[i] - Cl_{NO2-int}[i])\right) \quad (7)$$

Interface Mass Balance Equations (obtained by mass balance at the interface):

$$Cl_{NH4-int}[1..w] = \frac{S_{NH4}[i,1] \cdot D_{NH4} \cdot s/_{\delta} + Kla_2 \cdot Vw \cdot Cl_{NH4}[i]}{D_{NH4} \cdot s/_{\delta} + Vw \cdot Kla_2} \quad (8)$$

$$Cl_{NO2-int}[1..w] = \frac{S_{NO2}[i,1] \cdot D_{NO2} \cdot s/_{\delta} + Kla_2 \cdot Vw \cdot Cl_{NO2}[i]}{D_{NO2} \cdot s/_{\delta} + Vw \cdot Kla_2} \quad (9)$$

Biofilm Mass Balance Equations, where concentrations are written as S[vertical segment, horizontal segment]:

$$\frac{d}{dt}S_{NH4}[1..w,1] = \frac{D_{NH4} \cdot s}{\delta \cdot Vbn} \cdot (Cl_{NH4-int}[i] - 2 \cdot S_{NH4}[i,1] + S_{NH4}[i,2]) - R_{NH4}[i,1] \quad (10)$$

$$\frac{d}{dt}S_{NH4}[1..w,2..n-1] = \frac{D_{NH4} \cdot s}{\delta \cdot Vbn} \cdot (S_{NH4}[i,j-1] - 2 \cdot S_{NH4}[i,j] + S_{NH4}[i,j+1]) - R_{NH4}[i,j] \quad (11)$$

$$\frac{d}{dt}S_{NH4}[1..w,n] = \frac{D_{NH4} \cdot s}{\delta \cdot Vbn} \cdot (S_{NH4}[i,j-1] - S_{NH4}[i,j]) - R_{NH4}[i,j] \quad (12)$$

$$\frac{d}{dt}S_{NO2}[1..w,1] = \frac{D_{NO2} \cdot s}{\delta \cdot Vbn} \cdot (Cl_{NO2-int}[i] - 2 \cdot S_{NO2}[i,1] + S_{NO2}[i,2]) + R_{NH4}[i,1] \quad (13)$$

$$\frac{d}{dt}S_{NO2}[1..w,2..n-1] = \frac{D_{NO2} \cdot s}{\delta \cdot Vbn} \cdot (S_{NO2}[i,j-1] - 2 \cdot S_{NO2}[i,j] + S_{NO2}[i,j+1]) + R_{NH4}[i,j] \quad (14)$$

$$\frac{d}{dt}S_{NO2}[1..w,n] = \frac{D_{NO2} \cdot s}{\delta \cdot Vbn} \cdot (S_{NO2}[i,j-1] - S_{NO2}[i,j]) + R_{NH4}[i,j] \quad (15)$$

Table 1: Model parameter values and sources for the biotrickling filter model

Constant	Variable	Value	Source
G	Gas Flow Rate	1.27 to 2.83 m^3/h	Lab determined
E	Porosity	0.8	
Vw	Volume of one horizontal layer	0.003 m^3	Calculated
C_{inlet}	Inlet gas concentration	0.053 to 0.105 g/m^3	Lab determined
C	Gas Concentration	Model output	
Kla_1	Gas-Liquid Mass Transfer Coefficient	2100 h^{-1}	Calculated
kH	Henry's constant	6.7 x 10^{-4} (unitless)	(Baquerizo et al., 2005)
Cl_{NH4}	Liquid NH_4^+ concentration	Model Output	
L_{BTF}	BTF liquid flow rate	10 to 20 L/d	Lab determined
$Influent_{NH4}$	Influent Liquid NH_4^+ Concentration	0	Lab determined
Kla_2	Liquid-biofilm Mass Transfer Coefficient	0.096 h^{-1}	Calculated
$Cl_{NH4\text{-}int}$	Interface Liquid NH_4^+ concentration	Model output	
Vlw	Volume of liquid in one horizontal layer	2.98 x 10^{-4}	Calculated
$Influent_{NO2}$	Influent Liquid NO_2^- Concentration	0	Lab determined
Cl_{NO2}	Liquid NO_2^- Concentration	Model output	
$Cl_{NO2\text{-}int}$	Interface Liquid NO_2^- Concentration	Model output	
S_{NH4}	NH_4^+ Biofilm Concentration	Model output	

D_{NH4}	Diffusion of NH_4^+ in the liquid phase	4.97×10^{-6} m^2/h	(Baquerizo et al., 2005)
s	Biofilm Surface Area	1.79 m^2	Calculated
δ	Biofilm Thickness	10^{-4} m	Calculated
S_{NO2}	NO_2^- Biofilm Concentration	Model output	
D_{NO2}	Diffusion of NO_2^- in the liquid phase	4.43×10^{-6} m^2/h	(Baquerizo et al., 2005)
Vbn	Volume of one Individual Biofilm segment	4.47×10^{-5}	Calculated
R_{NH4}	NH_4^+ to NO_2^- Reaction	Model output	

3.2.3 Anammox Model Development

Previous models have been developed for the anammox reactor. Cema et. al modeled the anammox process in a membrane bioreactor (MBR) as biofilm reactors have good biofilm retention, which can reduce the lengthy start up period associated with the slow growing anammox bacteria. The MBR was operated as a continuously stirred tank reactor (CSTR) and the developed model was based on the activated sludge model 1 (ASM 1) (Cema, Sochacki, Kubiatowicz, Gutwiński, & Surmacz-Górska, 2012). The ASM 1 predicts reactor performance of substrate removal, nitrification and denitrification using Monod kinetics. The model developed by Cema et al. was able to predict the effluent ammonium and nitrite concentrations after calibration. The difference in the experimental and model ammonium and nitrite concentrations were 0.5 g N/m and 0.2 g N/m. (Cema et al., 2012). Another modeling study was conducted on the coupling of a one stage ammonium removal process, called completely autotrophic nitrogen removal

over nitrite (CANON), and the anammox system. This system comprised of a biofilm reactor, and the developed model was based on the activated sludge model 3 (ASM 3) (Hao, Heijnen, & Van Loosdrecht, 2001). Given that the anammox bacteria in our study were grown on circular packing, forming a thin biofilm on the packing, and that many other studies have modeled the anammox as biofilm, the developed model for the anammox system was for a biofilm system.

A dynamic model representing the anammox bioreactor was developed based on the mass balance schematic shown in Figure 13. Note that when joined with the BTF model, the influent liquid feed was the effluent liquid from the BTF (Figure 13). The model considers a submerged upward flow of the liquid undergoing treatment, thus submerging the circular packing containing the anammox microbes. No diffusion of ammonium and nitrite into the biofilm occurs where both serve as substrate and are degraded to dinitrogen gas.

The following assumptions were made when developing the anammox mass balances:

1. Each individual circular packing piece is symmetrical so that only one half needs to be modeled. Biofilm completely covers all circular packing and has uniform thickness
2. The liquid phase in each discretized layer is ideally mixed

3. Nitrate production is neglected and does not interfere with the ammonium and nitrite degradation

Mass balance equations for ammonium and nitrite in the liquid layer, interface and biofilm were developed and can be found in Equations 16 through 28 below. All parameters referenced in the following equations can be found in Table 2 below.

Liquid Mass Balance Equations

$$\frac{d}{dt}(Cl_{an-NH4}[1]) = (\frac{L_{an}}{Vlp} \cdot (Influent_{NH4} - Cl_{an-NH4}[i]) - Kla_3 \cdot Vp \cdot (Cl_{an-NH4}[i] - Cl_{an-NH4-int}[i])) \quad (16)$$

$$\frac{d}{dt}(Cl_{an-NH4}[2..p]) = (\frac{L_{an}}{Vlp} \cdot (Cl_{an-NH4}[i-1] - Cl_{an-NH4}[i]) - Kla_3 \cdot Vp \cdot (Cl_{an-NH4}[i] - Cl_{an-NH4-int}[i])) \quad (17)$$

$$\frac{d}{dt}(Cl_{an-NO2}[1]) = (\frac{L_{an}}{Vlp} \cdot (Influent_{NO2} - Cl_{an-NO2}[i]) - Kla_3 \cdot Vp \cdot (Cl_{an-NO2}[i] - Cl_{an-NO2-int}[i])) \quad (18)$$

$$\frac{d}{dt}(Cl_{an-NO2}[2..p]) = (\frac{L_{an}}{Vlp} \cdot (Cl_{an-NO2}[i-1] - Cl_{an-NO2}[i]) - Kla_3 \cdot Vp \cdot (Cl_{an-NO2}[i] - Cl_{an-NO2-int}[i])) \quad (19)$$

Interface Mass Balance Equations

$$Cl_{an-NH4-int}[1..p] = \frac{S_{an-NH4}[i,1] \cdot D_{an-NH4} \cdot S_a / \delta_a + Kla_3 \cdot Vp \cdot Cl_{an-NH4}[i]}{D_{an-NH4} \cdot S_a / \delta_a + Vp \cdot Kla_3} \quad (20)$$

$$Cl_{an-NO2-int}[1..p] = \frac{S_{an-NO2}[i,1] \cdot D_{an-NO2} \cdot s_a / \delta_a + Kla_3 \cdot Vp \cdot Cl_{an-NO2}[i]}{D_{an-NO2} \cdot s_a / \delta_a + Vp \cdot Kla_3} \quad (21)$$

Biofilm Mass Balance Equations

$$\frac{d}{dt} S_{an-NH4}[1..p,1] = \frac{D_{an-NH4} \cdot s_a}{\delta_a \cdot Vbm} \cdot (Cl_{an-NH4-int}[i] - 2 \cdot S_{an-NH4}[i,1] + S_{an-NH4}[i,2]) - R[i,1] \cdot S_{an-NH4}[i,j] \quad (22)$$

$$\frac{d}{dt} S_{an-NH4}[1..p,2..m-1] = \frac{D_{an-NH4} \cdot s_a}{\delta_a \cdot Vbm} \cdot (S_{an-NH4}[i,j-1] - 2 \cdot S_{an-NH4}[i,j] + S_{an-NH4}[i,j+1]) - R[i,j] \cdot S_{an-NH4}[i,j] \quad (23)$$

$$\frac{d}{dt} S_{an-NH4}[1..p,m] = \frac{D_{NH4} \cdot s_a}{\delta_a \cdot Vbm} \cdot (S_{an-NH4}[i,j-1] - S_{an-NH4}[i,j]) - R[i,j] \cdot S_{an-NH4}[i,j] \quad (24)$$

$$\frac{d}{dt} S_{an-NO2}[1..p,1] = \frac{D_{an-NO2} \cdot s_a}{\delta_a \cdot Vbm} \cdot (Cl_{an-NO2-int}[i] - 2 \cdot S_{an-NO2}[i,1] + S_{an-NO2}[i,2]) - R[i,1] \cdot S_{an-NO2}[i,j] \quad (25)$$

$$\frac{d}{dt} S_{an-NO2}[1..p,2..m-1] = \frac{D_{an-NO2} \cdot s_a}{\delta_a \cdot Vbm} \cdot (S_{an-NO2}[i,j-1] - 2 \cdot S_{an-NO2}[i,j] + S_{an-NO2}[i,j+1]) - R[i,j] \cdot S_{an-NO2}[i,j] \quad (26)$$

$$\frac{d}{dt} S_{an-NO2}[1..p,m] = \frac{D_{an-NO2} \cdot s_a}{\delta_a \cdot Vbm} \cdot (S_{an-NO2}[i,j-1] - S_{an-NO2}[i,j]) - R[i,j] \cdot S_{an-NO2}[i,j] \quad (27)$$

Reaction Kinetics Equation

$$R[1..p,1..m] = R_{max} \cdot \frac{S_{an-NH4}[i,j]}{K_{NH4} + S_{an-NH4}[i,j]} \cdot \frac{S_{an-NO2}}{K_{NO2} + S_{an-NO2}[i,j]} \quad (28)$$

Table 2: Model parameter values and sources for the anammox model

Constant	Variable	Value	Source

Vp	Volume of one horizontal layer	0.19 m^3	Calculated
Kla_3	Liquid-biofilm Mass Transfer Coefficient	9.8 x 10^{-4}	Calculated
Cl_{an-NH4}	Anammox Liquid NH_4^+ concentration	Model output	
Lan	Anammox liquid flow rate	6 to 16 L/d	Lab determined
$Influent_{NH4}$	Influent Liquid NH_4^+ Concentration	60 to 280 mg N/L	Lab determined
$Cl_{an-NH4-int}$	Interface Liquid NH_4^+ concentration	Model output	
Vlp	Volume of one horizontal liquid layer	0.005 m^3	Calculated
$Influent_{NO2}$	Influent Liquid NO_2^- Concentration	91 to 266 mg N/L	Lab determined
Cl_{an-NO2}	Liquid NO_2^- Concentration	Model output	
$Cl_{an-NO2-int}$	Interface Liquid NO_2^- Concentration	Model output	
S_{an-NH4}	NH_4^+ Biofilm Concentration	Model output	
D_{an-NH4}	Diffusion of NH_4^+ in liquid	5.76 x 10^{-6} m^2/h	(Ni et al., 2009)
S_a	Biofilm Surface Area	4.9 x 10^{-4}	Lab determined
δ_a	Biofilm Thickness	3 x 10^{-4}	Lab determined
S_{an-NO2}	NO_2^- Biofilm Concentration	Model output	
D_{NO2}	Diffusion of NO_2^- in liquid	5.83x10^{-6} m^2/h	(Ni et al., 2009)
Vbm	Volume of one Individual Biofilm Segment	0.19 m^3	Calculated

To determine the value of the reaction rate for the removal of ammonia and nitrite by the anammox microbes, 57 packing rings from the anammox reactor were placed in a small mason jar filled 0.7 L of effluent water collected from the BTF. The jar

was placed on a stir plate in an anaerobic chamber. Periodically over 6.5 hours, water samples were collected and analyzed for pH, nitrite, ammonium and nitrate. The pH was determined using a pH probe while the nitrite, ammonium and nitrate were analyzed using Hach test kits. Upon the completion of the experiment, the collected data was imported into Berkeley Madonna and the Monod kinetic parameters, specifically the maximum rate of consumption and the half-saturation constants, were determined using a curve fit. Monod kinetics were selected as previous research has modeled anammox substrate consumption using Monod kinetics and in activated sludge models, all biological growth is determined from Monod kinetics (M Strous, Kuenen, & Jetten, 1999). The maximum rate of consumption, R_{max}, and saturation constants, K_{NH4} and K_{NO2}, are listed below in Table 3.

Table 3: Experimentally determined anammox Monod kinetics parameters

Parameter	Value
R_{max}	1458 g/m^{3}hr
K_{NH4}	0.34 g/m^3
K_{NO2}	3.95 g/m^3

Cema et al. determined the Monod kinetic parameters via model calibration. They found the half saturation constants for ammonium and nitrite to be 0.08 and 2 g N/m^3 (Cema et al., 2012). While the half saturation constants found in this study differ

slightly, they are similar in that the half saturation constant for nitrite is significantly larger than that of the ammonium.

3.3 Model Validation

3.3.1 Biotrickling Filter Model Validation

Experimental data was used to determine mass transfer coefficients and kinetic parameters for the BTF model. The curve fitting feature in Berkley Madonna was used to adjust the kinetic parameters and liquid mass transfer coefficient so that the model best fit the experimental data. The adjusted R value, ammonium half saturation coefficient and the liquid mass transfer coefficient were found to be 0.08 g N/h m^3, 1.5 g/m^3 and 0.096 h^{-1}, respectively. The comparison of the average experimental ammonium and nitrite concentrations to the model concentrations can be found in Figure 14 and Figure 15.

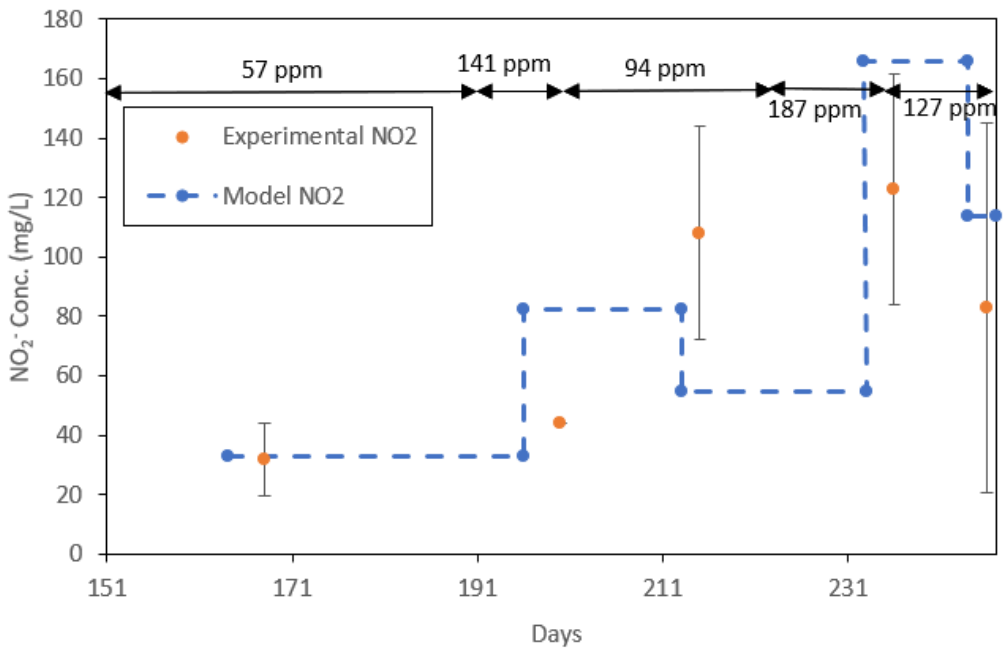

Figure 14: Comparison of model simulated and experimentally determined liquid effluent ammonium concentrations.

Figure 15: Comparison of model and average experimental liquid effluent nitrite concentrations.

Examination of Figures 14 and 15 reveals that the model more accurately represents nitrite concentrations than ammonium concentrations. The largest difference between experimental and model nitrite concentrations was 120 mg N/L or 98% whereas the largest difference between experimental and model ammonium concentrations was 136 mg N/L or 115%. On average both the modeled nitrite and ammonium concentrations tended to be lower than that of the experimental ones. It should also be noted that the modeled ammonium concentrations better showed the sensitivity in the

experimental data – i.e the change in the effluent ammonium concentrations due to the change in influent gas concentration was roughly the same for both the model and the experiment. This change is depicted in Figure 16.

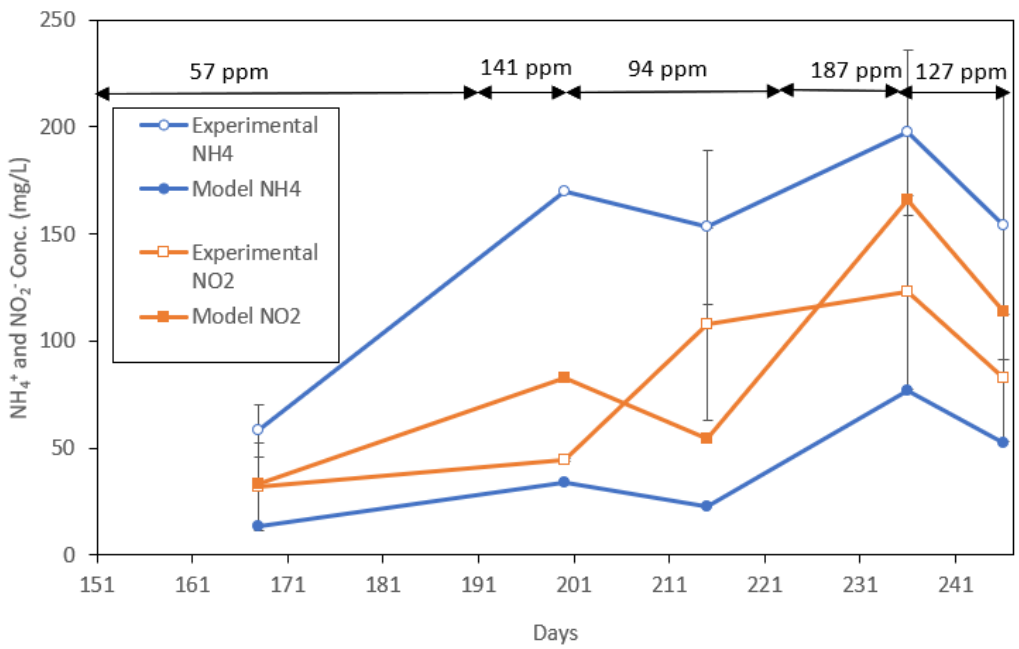

Figure 16: Comparison of the sensitivities in the average experimental and model ammonium and nitrite concentrations.

As mentioned, the model values for both nitrite and ammonium concentrations tended to be lower than that of the experiment for a variety of reasons. First, there was significant variability in the experimental ammonium and nitrite concentrations. This

occurred as the BTF was sensitive to pH fluctuations and often change in reactor loading conditions took a few days to become apparent in the effluent ammonium and nitrite concentrations. Additionally, the kinetic parameters used in the model were determined from previous studies and fitting to the experimental data. No specific laboratory experiment was conducted to determine these kinetic parameters. Microbial inhibition due to free nitrous acid (FNA) and oxygen limitation were also not considered but could have played a role (Park, Chung, Rittmann, & Bae, 2015). By not accounting for these inhibitions, the model showed better removal of nitrite and ammonium than achieved in the experiment.

3.3.2 Anammox Model Validation

The results generated by the anammox model at various influent flow rates (7, 8, 9, 11.2 and 16 L/d) and influent ammonium concentrations (60 to 280 mg N/L) and nitrite concentrations (91 to 266 mg N/L) were compared to their respective experimental values obtained in the lab (Figure 17 and Figure 18, respectively).

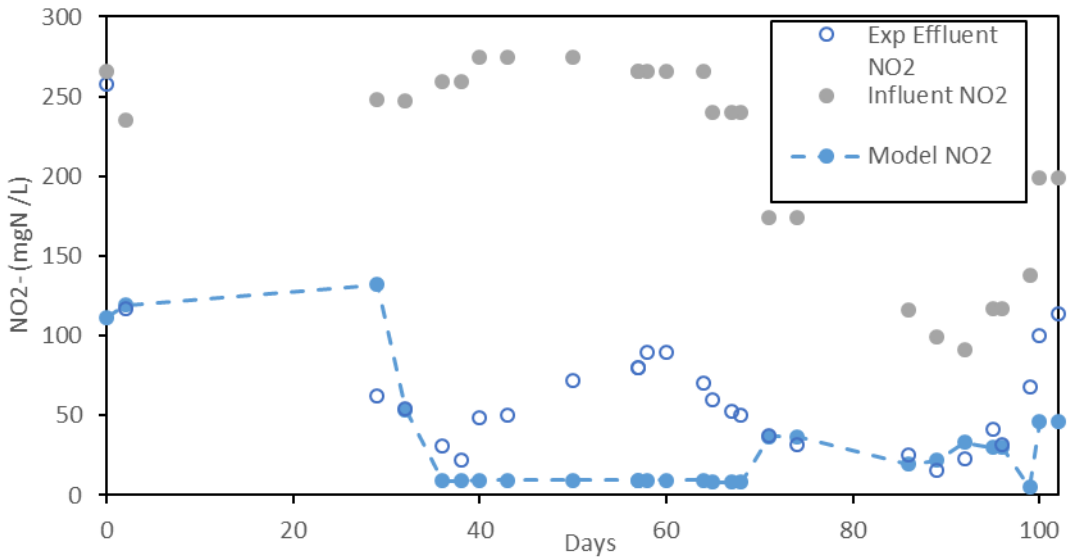

Figure 17: Comparison of model and experiment effluent nitrite concentrations at various influent flow rates.

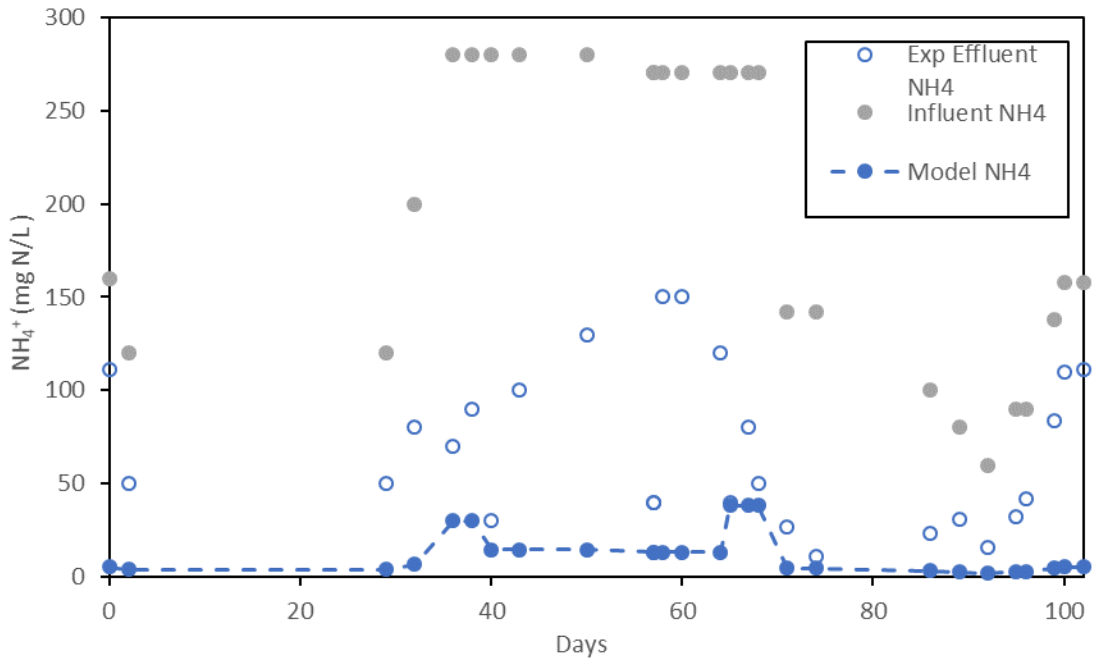

Figure 18: Comparison of model and experiment effluent ammonium concentrations at various influent flow rates.

Overall the developed model underestimated the effluent ammonium and nitrite concentrations by as much as 95% and 113%, respectively. On average, the model underestimated the effluent ammonium and nitrite concentrations by 77% and 59%, respectively. Additionally, both models did not closely match the experimental sensitivity to nitrogen loading as the model nitrogen removal above 90%. The discrepancy between the model and the experimental data is most likely due to model simplifications and assumptions. All the packing rings were assumed to be completely covered with biofilm, which would allow for higher removal. Additionally, any potential inhibition, whether it was due to high nitrite loading, the presence of oxygen,

the presence of nitrate, and non-optimal pH were not accounted for in the model. Further development of the model and incorporation of these factors should improve the model. A study conducted by Ni et al. developed a model for a granule based anammox process. When developing their model, they considered the anammox bacteria growth kinetics more in depth, and calibrated their model by adjusting the half saturation coefficients for ammonium and nitrite, the decay rate of the anammox bacteria and the yield of the anammox bacteria. After performing this calibration, the model developed by Ni et al. closely matched their experimental data (Ni et al., 2009). Perhaps incorporating more of the growth kinetics would improve the anammox model for this study.

3.3.3 Coupling of the biotrickling filter and anammox reactor models

The models were combined to provide an estimation of the overall system operation and to support optimization of the process. To combine the models, the simulated effluent liquid ammonium and nitrite values from the BTF model served as inputs into the anammox model. Simulations were repeated for various NH_3 loading rates to the BTF model and steady state performance were examined. The resulting nitrite and ammonium concentrations from the BTF and the anammox model are provided in Figure 19.

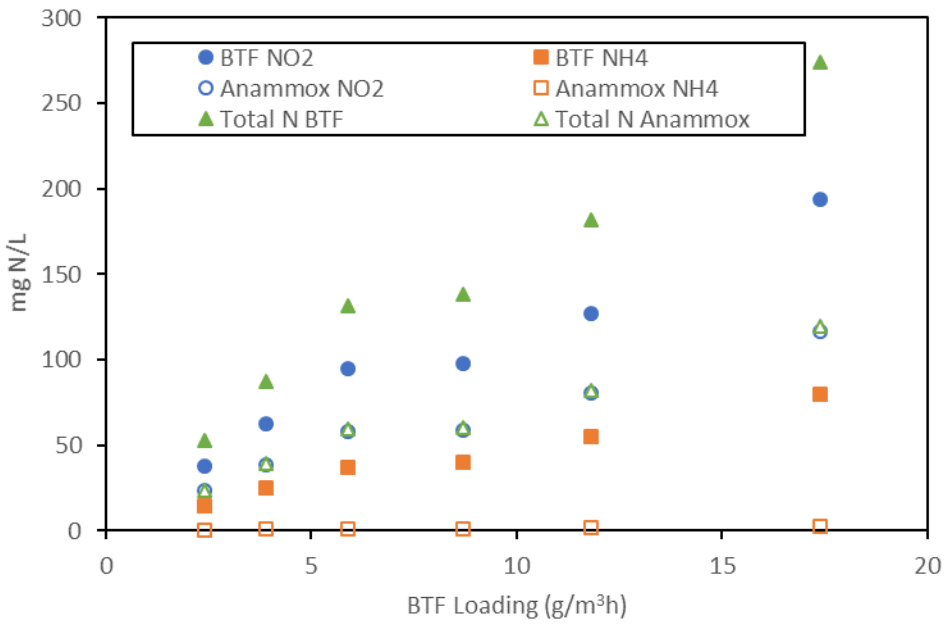

Figure 19: Effluent nitrite, ammonium and total nitrogen concentrations from the BTF and anammox model at various ammonia loading rates.

As shown in Figure 19, the BTF reactor provided influent ammonium and nitrite concentrations for the anammox reactor. The results provided in Figure 19 demonstrated that the anammox reactor was able to reduce the total nitrogen concentrations from the BTF effluent. The anammox model showed a significant reduction in the ammonium concentrations, the highest effluent ammonium concentration from the anammox reactor was 2.7 mg N/L. The effluent ammonium concentrations from the anammox model were lower than that of the nitrite concentrations as the BTF effluent ammonium concentrations were lower than the BTF effluent nitrite concentrations – the ammonium served as a limiting factor in the anammox reaction.

While the anammox reactor greatly reduced the ammonium concentrations from the BTF effluent, the nitrite concentrations were still slightly high – the highest total nitrogen in the anammox effluent was 119.6 mg N/L which occurred at a BTF loading of 17.4 g/m^{3}h. The combined anammox and BTF model was used to determine whether increasing the volume of the anammox reactor would improve the overall nitrogen removal from the anammox reactor. The results are provided in Figure 20.

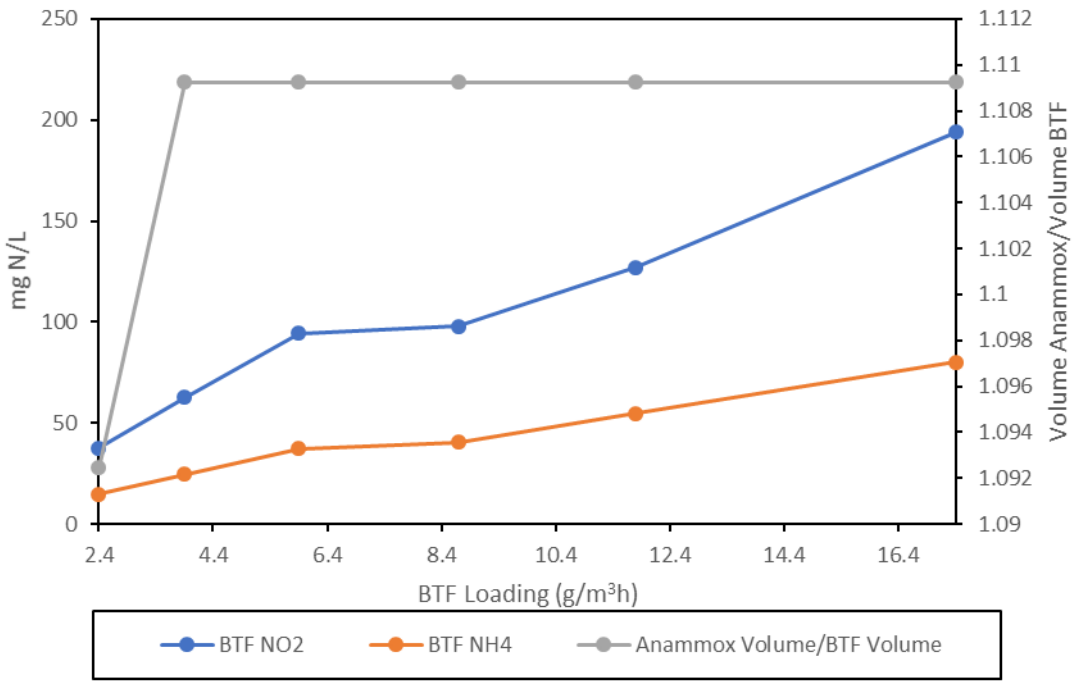

Figure 20: Anammox reactor volume to improve denitrification at various BTF loading rates.

To improve the denitrification (make it so that the nitrite removal was at least 90%) in the anammox reactor, the anammox reactor volume would need to be increased

so that it is approximately 1.1 times the volume of the BTF reactor. Little deviation in the required size of the anammox reactor existed for the various BTF loading rates. Increasing the volume of the anammox reactor resulted in a significant reduction in the effluent nitrite concentrations from the anammox reactor. There was a slight increase in the effluent ammonium concentrations using the larger anammox reactor volume compared to the original anammox volume. However, given that the effluent nitrite concentrations from the original anammox volume accounted for most of the total nitrogen in the effluent, the larger anammox reactor volume resulted in a reduced total nitrogen effluent concentration. The results are shown in Figure 21 below.

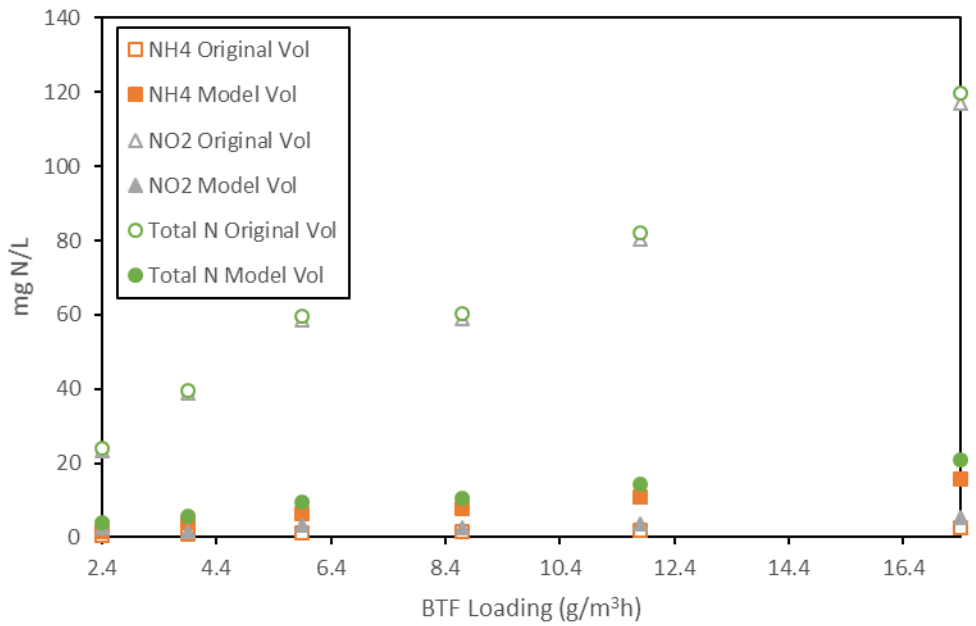

Figure 21: Effluent anammox nitrite, ammonium and total nitrogen concentrations for the current lab reactor volume and optimum model reactor volume.

As shown in Figure 21, increasing the anammox reactor volume resulted in a reduction in the total effluent nitrogen. The largest reduction in total effluent nitrogen, 98.6 mg N/L, occurred at a BTF loading of 17.4 g/m^{3}h. This result was expected as an increase in the anammox reactor volume would result in more biofilm and thus more denitrification.

4. Conclusion

Overall, the laboratory experiments showed that it is possible to achieve a nitrite to ammonium ratio close to 1 in the effluent of a BTF treating air contaminated with ammonia. To achieve this ratio the loading must be maintained at approximately 8.7

g/m^{3}h and the effluent pH must be between 6.5 and 7 unless a recycle line is added. This loading rate also resulted in complete (100%) ammonia gas removal. To obtain a nitrite to ammonium ratio of 1 with a recycle line, the recycle rate must be 1.4 times that of the influent mineral medium flow rate and the pH value can exceed 7. The anammox reactor was able to remove approximately 88% of the influent ammonium and nitrite at a loading rate of 10.5 g/m^{3}h. Given that a nitrite to ammonium ratio equal to 1 was achieved at a loading rate corresponding to complete ammonia gas removal this study suggests that the coupling of a BTF and anammox reactor to treat an ammonia gas stream is feasible. It has yet to be realized experimentally.

The developed model did not accurately simulate the performance of the lab scale BTF and anammox reactor. The model developed for the BTF underestimated the liquid effluent ammonium and nitrite concentrations obtained experimentally. The model slightly better predicted the nitrite concentrations than the ammonium concentrations. The largest difference between the model and experimental ammonium and nitrite concentrations was 115% and 98%, respectively. However, the model was able to accurately show the change in the liquid effluent ammonium concentrations resulting from change in the influent ammonia gas concentrations. The BTF model most likely overestimated the ammonium and nitrite concentrations as microbial inhibition due to oxygen limitation and FNA production was not incorporated. Incorporating these two factors may improve the BTF model. The model developed for the anammox

reactor underestimated the experimental effluent ammonium and nitrite concentrations. This underestimation most likely resulted from simplification of the model and assumptions made when developing the model.

Despite the discrepancies between model and experiments, the two models were combined to investigate the coupling of the BTF and anammox reactor. Six different BTF loading rates (2.4, 3.9, 5.9, 8.7, 11.8 and 17.4 g/m^{3}h) served as inputs to the BTF model. The resulting anammox effluent nitrogen concentrations showed that the effluent ammonium concentration was significantly lower than that of the nitrite. This occurred as the BTF effluent contained much higher nitrite concentrations than ammonium, making ammonium a limiting factor in the anammox model.

The combined BTF and anammox model was used to determine the optimum anammox volume reactor size to reduce the total nitrogen in the anammox effluent. Using the model, it was found that increasing the anammox reactor volume so that it was 1.109 times the volume of the BTF resulted in a significant reduction of the total effluent nitrogen from the anammox reactor.

4.1 Further Studies

While the lab experiments did prove the feasibility of using a BTF and anammox reactor to remove ammonia gas from an air stream, the loading of the BTF and anammox reactor were both relatively low. To have the potential to be used for

industrial purposes, the BTF and anammox system must be able to handle higher ammonia gas loading rates. For the BTF to handle higher loading rates while still producing a nitrite to ammonium ratio of 1 and achieve high removal rates, pH control may be necessary considering that nitrification decreases pH, while absorption of NH_3 increases it. Further research on optimizing nitrification rate and pH control in the BTF must be conducted. Additionally, the anammox reactor must be able to handle higher loading rates as well. Once loading exceeded 10 g/m^3h, the ammonium and nitrite removal dropped despite the fact that reports in the literature suggest that rates as high as 1.2 kg/m^3d could be obtained. Perhaps adding in a recycle line to the anammox reactor will improve removal efficiency.

Further research on the kinetics for the BTF and anammox reactor are necessary to improve the accuracy of the developed mathematical models. For the BTF, the model underestimated both the ammonium and nitrite concentrations. This underestimation most likely occurred due to non-inclusion of inhibition factors and using literature Monod kinetics rather than experimentally determined kinetics. The maximum R value used to calculate the ammonium consumption rate was determined by fitting the model to the experimental data. Experimentally determining these kinetic factors may improve the model fit and provide more validation on the selected kinetics. To improve the BTF model, inhibition factors such as inhibition caused by FNA and possibly oxygen limitation must be considered.

The anammox model underestimated both the ammonium and nitrite concentrations when comparing the model concentrations to those collected from the experiment. While lab experimentation was conducted to determine the kinetic parameters for the anammox model, the developed model was relatively simple. Perhaps including more in depth kinetics would improve the anammox model.

Appendix A

Table 4: Model parameters

Symbol	Parameter	Numerical Value	Units	Reference
n	Number of horizontal segments in BTF	5	NA	
w	Number of vertical segments in BTF	5	NA	
m	Number of vertical rows in anammox	10	NA	
p	Number of horizontal rows in anammox	10	NA	
L	Length of BTF	0.75	m	Lab determined
D	Diameter of BTF	0.1	m	Lab determined
L_{an}	Anammox liquid feed rate	Varied	m^3/hr	Lab determined
G	Gas flow rate	Varied	m^3/hr	Lab determined
C_{inlet}	Inlet Ammonia Concentration	Varied	g/m^3	Lab determined
O2_initial	Oxygen Concentration	275	g/m^3	Lab determined
V_{an}	Volume of anammox reactor	1.89×10^{-2}	m^3	Lab determined
L_{BTF}	BTF Liquid Feed Rate	Varied	m^3/hr	Lab determined
D_{NH4}	Diffusion of NH_4^+ in BTF	4.97×10^{-6}	m^2/h	(Baquerizo et al., 2005)
D_{NO2}	Diffusion of NO_2^- in BTF	4.43×10^{-6}	m^2/h	

KH	Henry's Constant for NH_3	$6.7x10^{-4}$	Unitless	
kg	Gas transfer coefficient	3.5	m/h	
kl	Liquid transfer coefficient	1.6×10^{-4}	m/h	(Texas, n.d.)
R	Used to Calculate Rmax	0.08	kgN/h m^3	Lab Determined
knh4	Half Velocity Constant for BTF	1.5	g/m^3	Lab Determined
R_{max}	Maximum ammonium and nitrite consumption rate in anammox	1458	1/hr	Lab Determined
K_{NH4}	Half Saturation Constant for Ammonium in anammox	0.34	g/m^3	Lab Determined
K_{NO2}	Half Saturation Constant for Nitrite in anammox	3.96	g/m^3	Lab Determined
$D_{an\text{-}NH4}$	Diffusion of NH_4^+ in anammox	$5.76x10^{-6}$	m^2/h	
$D_{an\text{-}NO2}$	Diffusion of NO_2^- in anammox	$5.83x10^{-6}$	m^2/h	(Ni et al., 2009)
diameter	Diameter of packing material in anammox	0.025	m	Measured
Thickness	Thickness of packing material in anammox	0.003	m	Measured
a	Specific surface area of BTF biofilm	600	m^2/m^3	
FT	Thickness of biofilm in BTF	$1x10^{-6}$	m	
$Volume_{rings}$	Total packing volume in anammox	0.008	m^3	Measured

V_{an}	Volume of anammox reactor	1.89×10^{-2}	M^3	Measured

Table 5: Calculated Model Parameters

Symbol	Parameter	Equation	Units
V_{BTF}	Total BTF volume	$L*(D/2)^2$ xpi	m^3
Vw	Volume of 1 horizontal reactor layer in BTF	V_{BTF}/w	m^3
s	Cross sectional area of biofilm in one layer of BTF	a x Vw	m^2
Vp	Volume of 1 horizontal reactor layer in anammox	V_{an}/p	m^3
δ	Thickness of one biofilm cell in BTF	FT /n	m
$V_{biofilm}$	Volume of biofilm in BTF	FT x s	m^3
Vbn	Volume of 1 biofilm piece in BTF	$V_{biofilm}/n$	m^3
Rmax_nh4	Max Specific Growth Rate	R/(a x FTn)x 1000	
Vlw	Volume of liquid layer in BTF	vl_percent x Vw	m^3
Vl_{an}	Volume of liquid in anammox	V_{an}-$Volume_{rings}$	m^3
Vlp	Volume of liquid layer in anammox	Vl_{an}/p	m^3
kla_1	Gas transfer coefficient in BTF	Kg x a	1/h
kla_2	Liquid transfer coefficient in BTF	Kl x a	1/h
Kla_3	Liquid transfer coefficient in anammox	Kl x a_a	1/h

Surface_area	Surface area of one packing ring in anammox	$(Diameter/2)^2$ x pi	m^2
δ_{an}	Thickness of one biofilm cell in anammox	Thickness/(2x m)	m
a_a	Specific surface area of anammox	Number*Surface_area*2	m^2/m^2
Number	Number of packing rings in anammox	$Volume_{rings}/(p*Volume_{biofilm})$	NA
$V_{biofilm}$	Volume of biofilm on 1 ring	Surface_area x Thickness	m^3
$V_{an\text{-}biofilm}$	Volume of biofilm in anammox in one horizontal layer	$Volume_{biofilm}$ x Number	m^3
Vbm	Volume of 1 biofilm piece in anammox	$V_{an\text{-}biofilm}/p$	m^3

References

Baquerizo, G., Maestre, J. P., Sakuma, T., Deshusses, M. A., Gamisans, X., Gabriel, D., & Lafuente, J. (2005). A detailed model of a biofilter for ammonia removal: Model parameters analysis and model validation. *Chemical Engineering Journal*, *113*(2–3), 205–214. https://doi.org/10.1016/j.cej.2005.03.003

Benjamin, Mark, M. (2010). Strong and Weak Acids, Ka, and Conjugate Acid/Base Pairs. In *Water Chemistry* (p. 136).

Cema, G., Sochacki, A., Kubiatowicz, J., Gutwiński, P., & Surmacz-Górska, J. (2012). Start-up, modelling and simulation of the anammox process in a membrane bioreactor. *Chemical and Process Engineering - Inzynieria Chemiczna i Procesowa*, *33*(4), 639–650. https://doi.org/10.2478/v10176-012-0054-6

Chen, W., Dai, X., Cao, D., Hu, X., Liu, W., & Yang, D. (2017). Characterization of a microbial community in an Anammox process using stored Anammox sludge. *Water (Switzerland)*, *9*(11), 1–11. https://doi.org/10.3390/w9110829

Groeneweg, J., Sellner, B., & Tappe, W. (1994). Ammonia Oxidation in Introsomonas at NH3 Concentrations near Km: Effects of pH and Temperature. *Water Research*, *28*(12), 2561–2566.

Hao, X., Heijnen, J. J., & Van Loosdrecht, M. C. M. (2001). Sensitivity analysis of a biofilm model describing a one-stage completely autotrophic nitrogen removal (CANON) process. *Biotechnology and Bioengineering*, *77*(3), 266–277. https://doi.org/10.1002/bit.10105

Melse, R.W; Ogink, N. W. . (2005). Air Scrubbing Techniques for Ammonia and Odor Reduction at Livestock Operations: Review of On-Farm Research in The Netherlands. *American Society of Agricultural Engineers*, *48*(6), 2303–2313.

Moussavi, G., Khavanin, A., & Sharifi, A. (2011). Ammonia removal from a waste air stream using a biotrickling filter packed with polyurethane foam through the SND process. *Bioresource Technology*, *102*(3), 2517–2522. https://doi.org/10.1016/j.biortech.2010.11.047

Ni, B. J., Chen, Y. P., Liu, S. Y., Fang, F., Xie, W. M., & Yu, H. Q. (2009). Modeling a

granule-based anaerobic ammonium oxidizing (ANAMMOX) process. *Biotechnology and Bioengineering*, *103*(3), 490–499. https://doi.org/10.1002/bit.22279

Niftrik, L. A. Van, Fuerst, J. A., & Damst, J. S. S. (2004). The anammoxosome : an intracytoplasmic compartment in anammox bacteria, *233*, 7–13. https://doi.org/10.1016/j.femsle.2004.01.044

Park, S., Chung, J., Rittmann, B. E., & Bae, W. (2015). Nitrite accumulation from simultaneous free-ammonia and free-nitrous-acid inhibition and oxygen limitation in a continuous-flow biofilm reactor. *Biotechnology and Bioengineering*, *112*(1), 43–52. https://doi.org/10.1002/bit.25326

Ramírez, M., Gómez, J. M., Aroca, G., & Cantero, D. (2009). Removal of hydrogen sulfide by immobilized Thiobacillus thioparus in a biotrickling filter packed with polyurethane foam. *Bioresource Technology*, *100*(21), 4989–4995. https://doi.org/10.1016/j.biortech.2009.05.022

Randall, D. J., & Tsui, T. K. . (2002). Ammonia Toxicity in Fish. *Marine Pollution Bulletin*, 17–23.

Sakuma, T., Jinsiriwanit, S., Hattori, T., & Deshusses, M. A. (2008). Removal of ammonia from contaminated air in a biotrickling filter - Denitrifying bioreactor combination system. *Water Research*, *42*(17), 4507–4513. https://doi.org/10.1016/j.watres.2008.07.036

Sancho, F. J. (2003). Biological Ammonia Removal.

Sri Shalini S, S. S., & Joseph, K. (2014). State of The Art Strategies for Successful ANAMMOX Startup and Development: A Review. *International Journal of Waste Resources*, *04*(04). https://doi.org/10.4172/2252-5211.1000168

Strous, M., Kuenen, J. G., & Jetten, M. S. M. (1999). Key physiology of anaerobic ammonium oxidation key physiology of anaerobic ammonium oxidation. *Applied and Environmental Microbiology*, *65*(7), 3248–3250.

Strous, M., Van Gerven, E., Zheng, P., Kuenen, J. G., & Jetten, M. S. M. (1997). Ammonium removal from concentrated waste streams with the anaerobic ammonium oxidation (anammox) process in different reactor configurations. *Water Research*, *31*(8), 1955–1962. https://doi.org/10.1016/S0043-1354(97)00055-9

Texas, U. of. (n.d.). Ionization constants for weak bases. Retrieved from http://www2.austin.cc.tx.us/chemlab/weakbase.htm

Xue, N., Wang, Q., Wu, C., Sun, X., & Xie, W. (2010). A pilot field-scale study on biotrickling filter treatment of NH3-containing odorous gases from organic waste composting plants. *Journal of Zhejiang University - Science A*, *11*(9), 629–637. https://doi.org/10.1631/jzus.A1000095